MOLECULAR AND CELLULAR BIOLOGY, Feb. 2007, p. 1017–1026 Vol. 27, No. 3
0270-7306/07/$08.00+0 doi:10.1128/MCB.01866-06

Murine Pif1 Interacts with Telomerase and Is Dispensable for Telomere Function In Vivo▽†

Bryan E. Snow,[1,2] Maria Mateyak,[3]‡ Jana Paderova,[2]‡ Andrew Wakeham,[1,2] Caterina Iorio,[1,2] Virginia Zakian,[3] Jeremy Squire,[2,4] and Lea Harrington[1,2,4]*

Campbell Family Institute for Breast Cancer Research, 620 University Avenue, Toronto, Ontario, Canada[1]; Ontario Cancer Institute, 610 University Avenue, Toronto, Ontario, Canada[2]; Princeton University, Lewis Thomas Laboratory, Princeton, New Jersey[3]; and Department of Medical Biophysics, University of Toronto, 610 University Avenue, Toronto, Ontario, Canada[4]

Received 2 October 2006/Returned for modification 29 October 2006/Accepted 10 November 2006

Pif1 is a 5′-to-3′ DNA helicase critical to DNA replication and telomere length maintenance in the budding yeast *Saccharomyces cerevisiae*. ScPif1 is a negative regulator of telomeric repeat synthesis by telomerase, and recombinant ScPif1 promotes the dissociation of the telomerase RNA template from telomeric DNA in vitro. In order to dissect the role of mPif1 in mammals, we cloned and disrupted the *mPif1* gene. In wild-type animals, *mPif1* expression was detected only in embryonic and hematopoietic lineages. *mPif1*$^{-/-}$ mice were viable at expected frequencies, displayed no visible abnormalities, and showed no reproducible alteration in telomere length in two different null backgrounds, even after several generations. Spectral karyotyping of *mPif1*$^{-/-}$ fibroblasts and splenocytes revealed no significant change in chromosomal rearrangements. Furthermore, induction of apoptosis or DNA damage revealed no differences in cell viability compared to what was found for wild-type fibroblasts and splenocytes. Despite a novel association of mPif1 with telomerase, mPif1 did not affect the elongation activity of telomerase in vitro. Thus, in contrast to what occurs with ScPif1, murine telomere homeostasis or genetic stability does not depend on *mPif1*, perhaps due to fundamental differences in the regulation of telomerase and/or telomere length between mice and yeast or due to genetic redundancy with other DNA helicases.

Homeostatic telomere length is achieved by a balance between the extension of the 3′ telomeric repeats by telomerase or by homologous recombination between telomeric tracts and telomere erosion due to incomplete DNA replication or nucleolytic degradation (30). Telomerase acts to lengthen telomeres via the reverse transcription of an RNA template (encoded by *TERC* in mammals or *TLC1* in *Saccharomyces cerevisiae*) by a telomerase reverse transcriptase (TERT or Est2, respectively) (30). In the absence of telomerase, telomeric repeats can also be maintained via homologous recombination (12). Excessive telomere lengthening is usually curtailed by *cis*-inhibitory telomere binding factors, such as Rif1 and Rap1 in *S. cerevisiae* and TRF1 in humans, or by the action of nucleases (30). In particular instances, telomeric tracts undergo saltatory attrition via the excision of telomeric DNA circles, thus preventing unregulated telomere lengthening (12, 40, 73).

This equilibrium is not simply a push and pull between factors that strictly promote or oppose telomere extension. In *S. cerevisiae*, the trimeric protein complex composed of Cdc13, Stn1, and Ten1 plays a critical role in the protection of chromosome ends from nucleolytic degradation, and the complex serves both positive and negative roles in the access of telomerase to the telomere during late S phase (24, 27, 66). The Ku70/Ku80 heterodimer, while essential for nonhomologous end joining, also plays a key role both in the recruitment of telomerase to the telomere and in the protection of ends from degradation (9, 25, 65, 74). Several DNA helicases and nucleases are also known to play key roles in the replication and maintenance of telomeres, including Pif1, Sgs1, Mre11, Rtel, and others (20, 34, 41).

Pif1 is a member of a 5′-to-3′ DNA helicase family whose other closest members include Rrm3 and, in *Schizosaccharomyces pombe*, Pfh1 (33, 37, 77). Unlike Rrm3 and Pif1, Pfh1 is essential (77). Rrm3 promotes the progression of replication forks at particular chromosomal loci prone to pausing during DNA replication (including the telomere), and *rrm3*Δ cells exhibit a modest telomere lengthening (11, 32, 33, 45, 59, 69). Mutation of ScPif1 leads to telomerase-dependent telomere lengthening (33, 76), and this phenotype depends on the ATP-unwinding activity of ScPif1; the enzyme has a preference for short (<30 nucleotides) RNA-DNA hybrids and can unwind telomerase RNA from a telomeric DNA substrate (15). Thus, Pif1 in *S. cerevisiae* inhibits telomerase elongation in vivo and in vitro. In humans, overexpression of active PIF1 leads to telomere shortening, and hPIF1 appears to reduce the elongation activity of telomerase in vitro, in a manner consistent with an effect on enzyme processivity (75).

Other roles for Pif1 may reflect a broader role for DNA-unwinding activity at the telomere and in nuclear and mitochondrial DNA replication. In the presence of double-stranded DNA breaks, chromosome ends are rarely healed by the de novo addition of telomeres (54). In the absence of nuclear ScPif1, gross chromosomal rearrangements are in-

* Corresponding author. Mailing address: Ontario Cancer Institute, Campbell Family Institute for Breast Cancer Research, 620 University Avenue, Room 706, Toronto M5G 2C1, Canada. Phone: (416) 946-2834. Fax: (416) 204-2277. E-mail: lea.harrington@oci.utoronto.ca.

† Supplemental material for this article may be found at http://mcb.asm.org/.

‡ These authors contributed equally.

▽ Published ahead of print on 27 November 2006.

creased, and healing of broken ends via telomere addition is more frequent (42, 47, 48, 61). Nuclear ScPif1 is also essential for mitigating the deregulated activity of the RecQ helicase Sgs1 observed in *top3*Δ cells (71). Interestingly, ScPif1 (but not Rrm3) colocalizes almost exclusively with Rad52 in nuclei and is recruited to discrete foci after DNA damage (71). ScPif1 and Rrm3 also play roles in the mitochondria, where they contribute to mitochondrial genome stability (21, 37, 51, 52, 67, 70). Finally, both ScPif1 and Pfh1 interact genetically with the Dna2 helicase and cooperate to ensure the correct processing of Okazaki fragments during DNA replication (17, 58).

We took a genetic approach to ascertain the role of Pif1 in mammals and disrupted the one putative murine homologue of ScPif1 and ScRrm3, called mPif1. We found that murine Pif1 expression was highly restricted and was detectable only in highly proliferating cells, such as embryonic stem (ES) cells and murine embryonic fibroblasts (MEFs), and in the hematopoietic lineage. In vitro, murine Pif1 interacted with telomerase activity in a telomerase RNA-independent manner. In *mPif1*-deficient animals, we found no evidence of sensitivity to DNA damage and no genetic instability, telomere length alteration, or other phenotypic abnormalities in cell types that would normally express Pif1. Moreover, *Pif1*-deficient animals exhibited normal life spans. These data suggest that that murine Pif1 is dispensable for normal telomere function, development, and aging in inbred mice.

MATERIALS AND METHODS

Cloning of murine Pif1. To isolate the cDNA encoding mPif1, oligonucleotide primers flanking the putative *mPif1* open reading frame were designed (sense primer 5′-TTG AAT TCC ACC ATG CGC TCC GGT CTC TGC ACG CCT GC-3′ [EcoRI Kozak] and antisense stop primer 5′-GCT GAG GTC AGA GGT TTG GGT CCA TGT TCT CC-3′) and used to amplify a 1.9-kb product from *c57Bl6* thymus cDNA. Reverse transcription-PCR amplifications were performed using Expand high-fidelity DNA polymerase (Boehringer Mannheim/Roche GmbH, Germany) according to the manufacturer's instructions and cloned into pCR2.1-TOPO (Invitrogen, San Diego, CA). After sequence verification, an EcoRI fragment spanning the entire mouse *Pif1* open reading frame was then subcloned into the mammalian expression vector pcDNA3.1+Zeo (Invitrogen), which was engineered with an N-terminal tandem hemagglutinin (HA) tag.

Construction of a murine *Pif1* targeting vector. In brief, PCR primers corresponding to the *mPif1* cDNA sequence (GenBank accession no. AY498715) (5′-GGG TAC CAG AAG GTG TTA GAT CTC CTG GAA CAC AAG GTT G-3′ [KpnI sense] and 5′-ACT CGA GCG GCC TGC TCT TCA GAA AGC TTC GGT TTG GTG G-3′ [XhoI antisense]) were used to amplify an ~3.4-kb long-arm fragment from 200 ng of 129J genomic DNA, using the Expand long-template PCR system (Roche GmbH, Germany). The Expand high-fidelity PCR system (Roche) was used to amplify a 771-bp short arm from 129J Genomic DNA, using the PCR primers 5′-ATC TAG ACC GTG TAT CAA CAC CAG CAT CCT ATT CCA GGT CTG C-3′ (XbaI sense) and 5′-CGC GGC CGC ACT GTC TAT AGC CTC AAA GCT GTG TAC ATC ACC TGG-3′ (NotI antisense). The resulting PCR products were gel purified using the QiaQuick gel purification system (QIAGEN Inc., Chatsworth, CA), TA cloned into pCR2.1 (Invitrogen, San Diego, CA), and subcloned into pBluescript II KS (Stratagene, La Jolla, CA) containing a phosphoglycerate kinase (PGK)-neomycin cassette. The insert sequence was obtained using fluorescent dideoxynucleotide sequencing and automated detection (ABI/Perkin Elmer, Forest City, CA).

Targeted disruption of the *mPif1* gene in ES cells. The *mPif1* targeting vector (25 μg) was linearized with the NotI restriction endonuclease at the short arm and electroporated into E14 ES cells (derived from the R129J strain). After G418 selection (300 μg/ml), homologous recombinants were identified by PCR and confirmed by Southern blot analysis, following published protocols (28). Primer mPIF1 Wt-1, which is specific for the region deleted in targeted *mPif1*, was used to detect the wild-type allele. Primer PGK-1, which is specific for the PGK promoter of the targeting construct, was used to detect the mutant allele. Primer mPIF1 Wt-2 was used to detect both the wild-type and mutant alleles of *mPif1*. The sequences are as follows: for mPIF1 Wt-1, 5′-GAG GCT GAT CTG ATG ACA GGA TAG CGA G-3′; for PGK-1, 5′-GCT GTC CAT CTG CAC GAG ACT AGT GAG ACG-3′; and for mPIF1 Wt-2, 5′-CAG GGC CTG GGA GTC AGC TCA CCA C-3′. A 912-bp probe flanking the 3′ end of the short arm of the targeting vector was used to confirm correct insertion by Southern analysis; this probe was generated by PCR amplification using the following primers: sense, 5′ TCT TCA TCG AGA GCC CTG ACA AGC AAC 3′; and antisense, 5′ CTG AGG AAG GCA TTG AGA AGT CCC ACC 3′.

Generation of *mPif1*-deficient mice and ES cells. Chimeric mice were produced by microinjection of independent *mPif1*$^{+/-}$ ES cell clones into E3.5 C57BL/6J blastocysts and transferred to ICR pseudopregnant foster mothers. The generation of founder *mPif1*$^{-/-}$ lines and breeding of homozygous-null animals were performed as previously described for *mTert*$^{-/-}$ animals (22, 38). The initial background is a mixture of 129J and C57BL/6J; therefore, to obtain *mPif1*$^{-/-}$ in a homogeneous background, the mixed-genetic-background *mPif1*$^{+/-}$ mice were bred for eight generations to C57BL/6 mice and then mated together to generate *mPif1*$^{-/-}$ mice (termed G_1, C57BL/6). Murine *Pif1*$^{-/-}$ ES cell clones were generated from G418-resistant *mPif1*$^{+/-}$ ES cell clones by culturing them with an increased G418 concentration (3.5 mg/ml). The ES cell culture was carried out as described previously (28).

Telomere length analysis. The average telomere fluorescence in populations of isolated splenocytes and thymocytes was measured by fluorescence in situ hybridization (FISH) (57) with minor modifications. A telomere-specific fluorescein isothiocyanate-conjugated $(CCCTAA)_3$ peptide nucleic acid probe (0.3 μg/ml) (Perseptive Biosystems) was used. Telomere fluorescence was expressed as numbers of molecules of equivalent soluble fluorochrome. Quantitative fluorescence in situ hybridization (Q-FISH) of activated splenocytes and MEFs was performed as described previously (14, 78). A Cy3-labeled $(CCCTAA)_3$ peptide nucleic acid (Applied Biosystems) was used as a probe. Chromosomes were counterstained with DAPI (4′,6′-diamidino-2-phenylindole). Telomere fluorescence signal intensities were quantified using TFL-Telo Q-FISH software (version 2.1.04.1217; BC Cancer Agency; Steven S. S. Poon and Peter M. Lansdorp). Telomere signal intensities were compiled from at least 10 metaphases (1,600 telomeres) for each sample. Metaphase images from littermates composed of all genotypes (the wild type, *mPif1*$^{+/-}$, and *mPif1*$^{-/-}$) were analyzed at the same time for technical consistency.

SKY. Spectral karyotyping (SKY) was performed on metaphase spreads from MEFs and splenocyte cells according to the manufacturer's instructions (Applied Spectral Imaging, Carlsbad, CA) and as previously published (4, 60). Metaphase cell spreads, selected for good-quality nonoverlapping chromosome spreads, were analyzed in a blinded manner with activated splenocyte samples from two different +/+, +/−, and −/− murine strains and primary MEF samples from one of each representative genotype (including two separately generated −/− lines). Samples were decoded after image analysis, and data acquisition was complete. According to the *I*nternational *S*ystem for Human *C*ytogenetic *N*omenclature (ISCN), karyotypes are normal unless a numerical gain is seen in at least two cells, a chromosomal loss seen in at least three cells, or a chromosomal rearrangement seen in at least two cells (44). DAPI analysis was also used to detect any numerical chromosomal or ploidy changes in MEFs and splenocytes. At least 20 metaphase spreads were analyzed in a blinded manner for at least one sample of each genotype.

Murine splenocyte cytogenetic preparation. Activated primary mouse splenocytes were isolated from C57BL/6 mice and cultured in RPMI 1640 media containing 10% (vol/vol) fetal calf serum (Sigma Aldrich Co.), 1% (wt/vol) L-glutamine, 0.55 mM β-mercaptoethanol, and 1% (wt/vol) penicillin-streptomycin (Gibco/BRL, Toronto, Canada). The splenocytes were activated with anti-CD3ε antibody (BD Biosciences) for 24 h and then transferred to media supplemented with interleukin 2 (BioSource) for an additional 24 h. The following day, the cultures were treated with 0.1 μg/ml Colcemid (Roche) for 5 to 6 h, swollen in 0.075 M KCl hypotonic buffer, fixed in a 3:1 volume of methanol-acetic acid, and dropped onto slides.

Murine MEF cytogenetic preparation. MEFs were cultured in Dulbecco's modified Eagle's medium-H21 medium containing 10% (vol/vol) fetal calf serum (Sigma Aldrich Co.), 1% (wt/vol) L-glutamine, 0.055 mM β-mercaptoethanol, and 1% (wt/vol) penicillin-streptomycin (Gibco/BRL, Toronto, Canada). Plates of approximately 80% confluent MEFs were processed in the same manner as the splenocytes except that they were treated with 0.05 μg/ml of Colcemid (Roche) for 3 to 4 h.

Cell viability in splenocytes and MEFs. Freshly isolated mouse splenocytes were harvested from three independent wild-type or *mPif1*$^{-/-}$ mice and stained with annexin V and 7-amino-actinomycin D according to the manufacturer's instructions (BD Biosciences). In brief, splenocytes were resuspended in binding

buffer containing annexin V-PE (to detect apoptosis) and 7-amino-actinomycin D (to detect necrosis) and then processed for flow cytometry analysis. For the analysis of cell viability in MEFs, cells from each genotype (+/+, +/−, or −/−) were seeded at 5×10^4 cells per well, in a total of six wells. The approximate doubling times were as follows: for 2919A, 37 h; for 2945B, 36 h; and for 2945D, 35 h. The R^2 values for the exponential curve fits are as follows: for 2919A, 0.9464; for 2945B, 0.9753; and for 2945D, 0.97. The experiment was carried out twice, and no statistical difference in growth rates was observed. For the analysis whose results are shown in Fig. S3B in the supplemental material, exponentially growing MEFs were trypsinized, and the cells were washed and fixed in ice-cold ethanol. For propidium iodide staining, the cells were precipitated and washed with phosphate-buffered saline containing 0.5% (vol/vol) fetal calf serum. The cell pellets were then resuspended in phosphate-buffered saline containing 0.5% (vol/vol) fetal calf serum, 8 μg/ml propidium iodide, and 125 μg/ml RNase A and incubated for 2 h at room temperature in the dark.

DNA damage response in MEFs. For the ionizing irradiation and UV light dose response curves, 6.7×10^4 passage 4 cells were plated per well in a total of six wells. The cells were treated with the indicated doses of either ionizing radiation or UV the following day. γ-Irradiation was administered via a ^{137}Cs source, and UV was administered via a Stratalinker (Stratagene). The cells were then cultured for 3 days, at which time the number of viable cells was determined, in triplicate, by trypan blue exclusion. For the hydroxyurea dose response curve, $\sim 1 \times 10^5$ passage 5 cells were plated per well in a six-well cluster. Cells were incubated at the indicated concentrations of hydroxyurea for 24 h. The cells were then washed to remove the drug and incubated for 2 days, at which time the number of viable cells was determined, in triplicate, by trypan blue exclusion.

Generation of anti-mPif1 antibody. A cDNA fragment encoding the N-terminal 216 amino acids (aa) of mPif1 (aa 1 to 216) was subcloned in-frame with both an amino- and a carboxyl-terminal six-histidine tag into the bacterial expression vector pET30b (Novagen, Madison, WI), purified, and injected into New Zealand White rabbits (University of Toronto). Antibody was affinity purified by incubating 0.5 ml of crude rabbit serum with 200 μg of the same purified mPif1 N-terminal antigen immobilized onto a nitrocellulose filter and eluting the specifically bound antibodies with 50 mM glycine-HCl (pH 2.7). The specificity of this polyclonal antibody was confirmed by Western blot analysis using full-length mPif1 in vitro transcribed and translated in rabbit reticulocytes (Promega) or cell extracts from human 293T cells overexpressing recombinant mPif1.

In vitro transcription and translation. In vitro transcription/translation reactions were performed using the TnT T7 coupled-reticulocyte-lysate system (Promega, Madison, WI) according to the manufacturer's instructions. The reconstitution of murine or human telomerase was performed as described previously (6, 7). The reaction mixtures were then immunoprecipitated with 25 μl of a 50% (vol/vol) slurry of either anti-HA (3F10) agarose beads (Roche), anti-Flag beads (Sigma Aldrich Co.), or protein A-Sepharose-CL4B (Sigma Aldrich Co.) coupled with polyclonal antibody, washed, and resolved as described previously (6, 7). Western blots were probed with anti-HA (3F10), anti-mPif1, or anti-TERT antibody and detected by chemiluminescence (Amersham Pharmacia).

Cell transfection, immunofluorescence, and immunoprecipitation. HA-tagged full-length mPif1 was transfected alone into human 293T cells with FuGene6 (Roche). Exponentially dividing 293T cells transiently expressing vector alone or HA-mPif1 were grown on two-well chamber slides coated with 0.1 mg/ml poly-L-lysine (Sigma, St. Louis, MO), fixed for 10 min in 4% (wt/vol) paraformaldehyde, and stained with DAPI or with affinity purified polyclonal anti-mPif1 primary antibody and an Alexafluor-488 anti-rabbit immunoglobulin G secondary antibody (Molecular Probes). For detection by immunoprecipitation, whole-cell lysis was carried out using 1:4 cell pellet volumes of 0.5% (wt/vol) 3-[(3-cholamidopropyl)-dimethylammonio]-1-propanesulfonate (CHAPS), in a buffer containing 10 mM Tris-HCl (pH 7.5), 1 mM $MgCl_2$, 0.1 M NaCl, 5 mM β-mercaptoethanol, and 10% (vol/vol) glycerol. Approximately 1 mg of cell or tissue protein extract was subjected to immunoprecipitation with the appropriate antibody in CHAPS buffer. Beads were washed in the same buffer four times before they were examined by Western analysis.

TRAP. The telomere repeat amplification protocol (TRAP; Intergen, Inc.) was carried out according to the manufacturer's instructions, with minor modifications (35). A cell extract or a portion of beads following immunoprecipitation (typically 2 to 4 μl) was assayed for the presence of telomerase activity. A titration of the cell extract was used to demonstrate that the TRAP products were in the near-linear range.

RESULTS

Cloning and expression analysis of murine Pif1. We cloned a cDNA encoding a putative murine ortholog of *S. cerevisiae* Pif1, called mPif1. The protein consists of 650 amino acids with a predicted molecular mass of 71 kDa and shows 85% and 93% amino acid identity to human and rat Pif1, respectively (Fig. 1). Although mPif1 shows amino acid sequence similarity to both ScPif1 and ScRrm3 (25% identity to each), we refer to the protein as mPif1. A BLAST search of the *c*onserved *d*omain *d*atabase (CDD) (43) at the NCBI identified a helicase domain spanning amino acids 214 to 613 (motifs I through V). This domain is most similar to the *Escherichia coli* RecD helicases, which comprise an ATP-dependent bacterial helicase superfamily I member which functions in DNA replication, recombination, and repair (10, 13, 46). There is also a large region of conservation between helicase motifs IV and V (amino acids 392 to 528) of the mouse Pif1 protein (Fig. 1A and B). The CDD identifies this conserved region as a DUF889 domain. DUF889 is a eukaryotic protein of an unknown function. The majority of members containing this domain are described as putative helicases.

To determine the tissue-specific distribution of the *mPif1* mRNA, we performed Northern analysis on RNA prepared from different adult and embryonic mouse tissues and cell lines. Hybridization of a full-length *mPif1* cDNA probe (GenBank accession no. AY498715) to poly(A)$^+$ RNA prepared from various adult mouse tissues showed a single transcript of ~4.0 kb present in adult thymuses and in all embryonic tissues and cell lines analyzed (Fig. 2B). The ~4-kb mRNA corresponds well with the predicted 3.68-kb full-length *mPif1* cDNA (GenBank accession no. AY498715), taking into account a typical poly(A) tail of ~200 residues for mature vertebrate mRNAs (72).

Disruption of murine Pif1. A targeting construct was designed to delete a region of mPif1 that spanned the first five conserved helicase motifs of *mPif1* (Fig. 2A), starting near the end of exon 3 (corresponding to aa 222) and deleting the next five exons (until aa 407), including deletion of a lysine at aa 243 of mPif1, which is predicted to be essential for activity (36). Exons 1, 2, and 8 to 13 remained intact. Note that the neomycin phosphotransferase gene in the disruption cassette is transcribed in a direction opposite that of *mPif1*, thus decreasing the likelihood of a partial *mPif1* transcript after targeted deletion. The linearized *mPif1* vector was introduced into E14 (wild-type) ES cells, and after selection in G418, homologous recombinants were identified by PCR and confirmed by Southern blot analysis. Chimeric mice and founder mice were generated as described in Materials and Methods. Germ line transmission of the mutant allele was confirmed by PCR and Southern blot analysis (Fig. 2A). Murine *Pif1*$^{-/-}$ ES cell clones were generated from G418-resistant *mPif1*$^{+/-}$ ES cell clones by incubation at an increased G418 concentration (Fig. 2A). Northern analysis of *mPif1*$^{-/-}$ embryonic stem cells, MEFs, and thymocytes confirmed the complete absence of the *mPif1* transcript (Fig. 2B, right).

To determine the tissue distribution of mPif1 protein and confirm its absence in *mPif1*$^{-/-}$ cells, we generated an antibody to mPif1 (see Fig. S1 in the supplemental material). This antibody was specific to mPif1 expressed in *E. coli*, rabbit

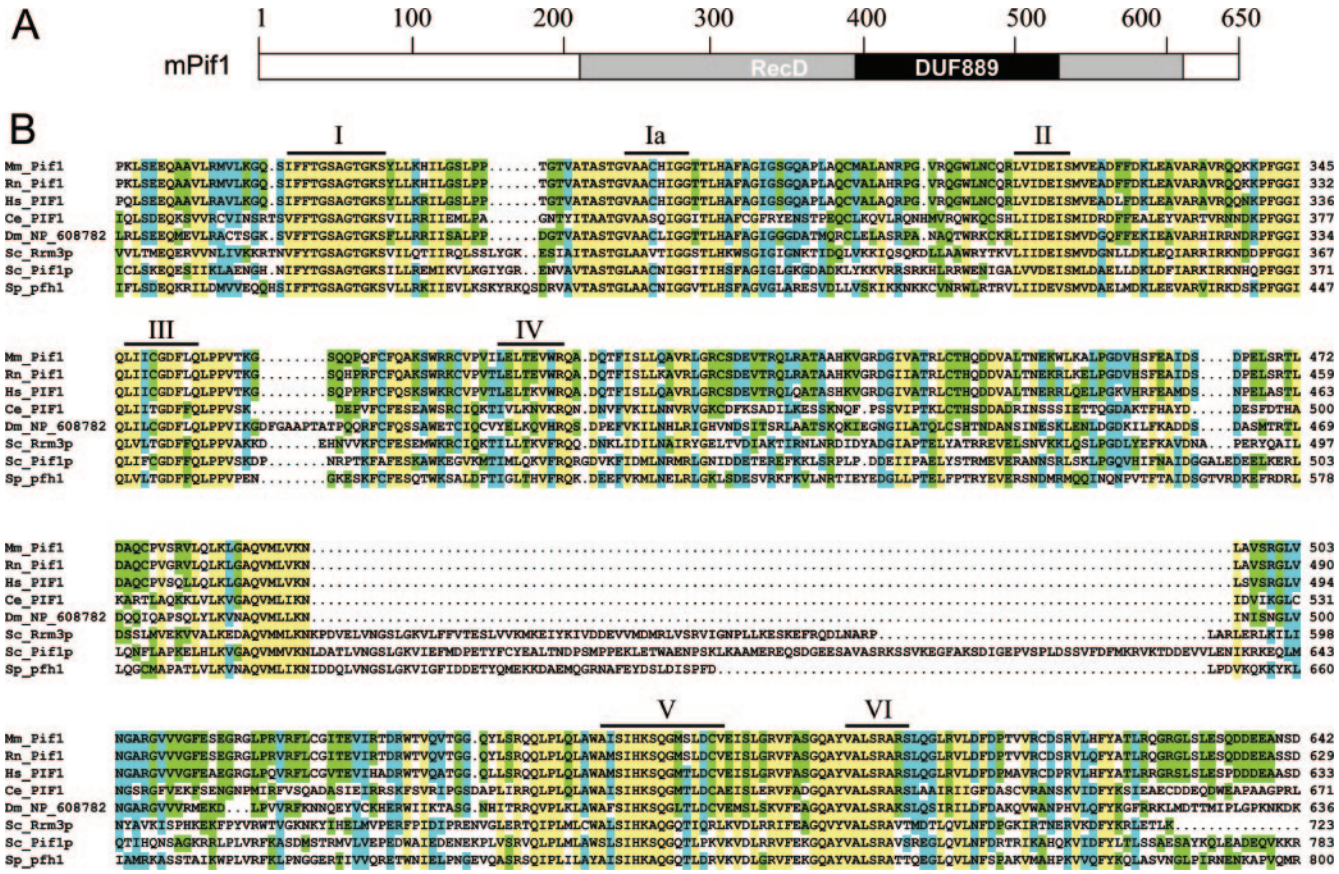

FIG. 1. Domain structure and amino acid alignment of mPif1. (A) Schematic of the domain structure of mouse Pif1 as identified by the CDD (43) at the NCBI. The major *E. coli* RecD helicase domain is shown in gray. The DUF889 domain (between helicase motifs IV and V) is shown in black. (B) Multiple sequence alignment of the RecD helicase domains of Pif1 homologues from selected species *Caenorhabditis elegans* (Ce), *Drosophila melanogaster* (Dm), *Homo sapiens* (Hs), *Mus musculus* (Mm), *Rattus norvegicus* (Rn), *S. cerevisiae* (Sc), and *S. pombe* (Sp). The alignment was shaded in conservation mode using GeneDoc (version 2.6) according to the following amino acid property similarity groups: aliphatic (AVILM), aromatic (FWYH), acids and amides (QEDN), positive (KR), and tiny (SGA). Residues showing 100% conservation are shaded yellow, those showing 80% to 90% conservation are shaded blue, and those showing 50% to 80% conservation are shaded green. The seven conserved helicase motifs, as defined for superfamily I by Gorbalenya and Koonin (1993) (26) and for the Pif1 subfamily by Bessler et al. (2001) (10), are indicated in roman numerals and represented by black bars above the sequences. Amino acid residue numbers are indicated for each respective protein.

reticulocyte lysates, and 293 cells (see Fig. S1A to C in the supplemental material). Overexpressed mPif1 was detected in 293 cell nuclei; however, the antibody was insufficiently sensitive to detect endogenous mPif1 by immunofluorescence (see Fig. S1C in the supplemental material; also data not shown). A large-scale immunoprecipitation followed by western analysis, using the mPif1 antibody, revealed a faint species at ~64 kDa that was present in wild-type and *mPif1*$^{+/-}$ ES cells but absent in *mPif1*$^{-/-}$ cells (see Fig. S1B in the supplemental material). Both recombinant mPif1 and the putative endogenous mPif1 species migrated slightly faster (~65 kDa) than predicted by its molecular mass of 71 kDa.

Telomere length analysis of *mPif1*$^{-/-}$ mice. To analyze the consequences of *mPif1* deletion upon the length distribution of mammalian telomeres, we mated *mPif1*$^{-/-}$ animals (as cousins, to prevent spurious effects from unlinked loci) for multiple generations both in the mixed genetic background from which the original knockout strain was derived and after backcrossing *mPif1*$^{+/-}$ animals into a pure C57BL/6 background. Telomere length was assessed by flow cytometry of fixed cellular DNA hybridized to a fluorescent telomeric probe (flow-FISH) (3) and quantitative measurement of fluorescent telomeric signal at each chromosome end in metaphase preparations (Q-FISH) (Fig. 3 and data not shown) (3). No change in telomere length was observed in *mPif1*$^{-/-}$ ES cells for up to 100 population doublings (Fig. 3A). In the original mixed genetic background, a statistically significant increase in telomere length was observed in one *mPif1*$^{-/-}$ litter after four generations; however, this increase was not reproduced in other litters and was no longer evident after five and six *mPif1*$^{-/-}$ generations (data not shown). After *mPif1*$^{-/-}$ mice were backcrossed into a pure C57BL/6 background, telomere lengths were again analyzed in successive *mPif1*$^{-/-}$ generations. No difference in average telomere DNA content or telomere length distribution was observed in *mPif1*$^{-/-}$ thymocytes or splenocytes for up to four generations (Fig. 3B). Similar results were also obtained after five and six generations in the *mPif1*$^{-/-}$ background (data not shown). Thus, in stark contrast to the telomere-lengthening

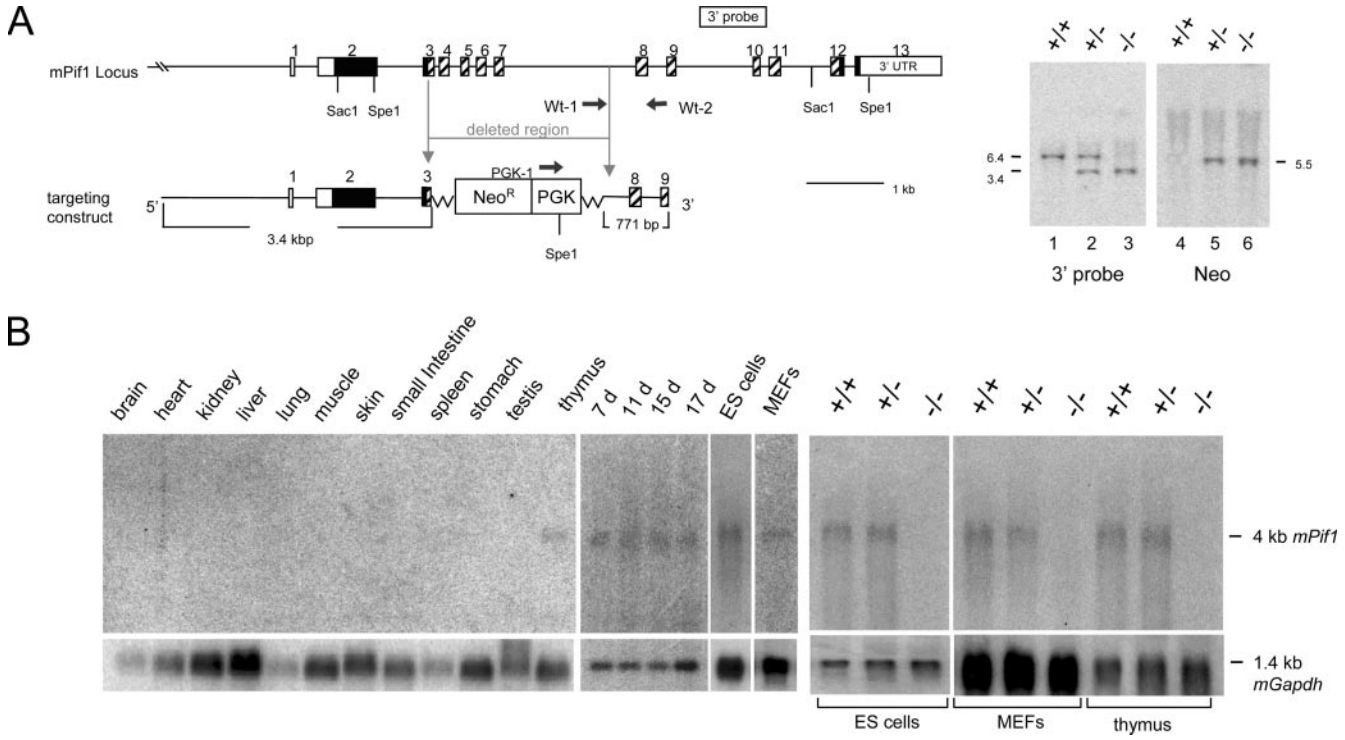

FIG. 2. Disruption of the *mPif1* locus in ES cells and mice. (A) Left, schematic representation of the endogenous *mPif1* locus and the targeting vector. Boxes represent exons, and hatched boxes represent exons corresponding to the conserved RecD helicase domain. Homologous recombination results in the insertion of a new SpeI site into the targeted locus and allows the targeted and wild-type alleles to be distinguished by Southern blot analysis with the indicated 3′ probe or by PCR using primers WT-1, WT-2, and PGK-1. Neo^R, neomycin phosophotransferase. Right, detection of targeted and wild-type *mPif1* alleles by Southern blot analysis of DNA from G_1 *mPif1*$^{-/-}$ mice. DNA was digested with SpeI and hybridized with the 3′ probe shown in panel A. In the left panel, the 6.4-kbp SpeI fragment corresponding to the wild-type allele is decreased to 3.4 kbp upon disruption of the locus. The adjacent panel shows the same samples digested with SacI and hybridized with a probe specific for the Neo^r gene to confirm a single integration event. (B) Northern analysis of *mPif1*. Left panel, two micrograms of poly(A)$^+$ RNA from various adult mouse tissues, tissue from embryonic days 7 to 17, ES cells, and MEFs. Right panel, Northern blot of *mPif1* transcripts from poly(A)$^+$ RNA isolated from wild-type, *mPif1*$^{+/-}$, and *mPif1*$^{-/-}$ ES cells, MEFs, and adult thymuses. Blots were hybridized with a full-length ^{32}P-labeled *mPif1* cDNA probe (top) or a murine glyceraldehyde 3-phosphate dehydrogenase (*Gapdh*) cDNA (bottom).

phenotype of cells lacking nuclear Pif1 in *S. cerevisiae*, no change in telomere length was observed for up to six generations of *mPif1*$^{-/-}$ mice.

Chromosome stability and cell viability in *mPif1*$^{-/-}$ cells. In *S. cerevisiae*, the absence of Pif1 dramatically increases the rate of gross chromosomal rearrangements. Although no gross genomic rearrangements were evident in DAPI-stained metaphase preparations under any of the conditions that we examined (Fig. 2A and data not shown), we nonetheless performed a detailed analysis of chromosome ploidy and gross chromosome rearrangements in *mPif1*$^{-/-}$ MEFs and splenocytes, using SKY. Chromosome rearrangements were observed in all three genotypes at a low frequency. Despite an apparently decreased number of chromosomal aberrations in *mPif1*$^{-/-}$ MEFs and splenocytes, there was no reproducible statistically significant change in chromosome gain/loss or rearrangements as assessed by chi-square analysis (Table 1, Fig. S2 in the supplemental material, and data not shown). Since replication-induced DNA damage can activate an intra-S-phase checkpoint, we also examined the cell cycle distribution of asynchronously dividing *mPif1*$^{-/-}$ cells. Splenocytes from *mPif1*$^{-/-}$ mice, when activated in vitro, revealed no differences in cell viability or distribution in the cell cycle (see Fig. S3A in the supplemental material). Similarly, early-passage primary *mPif1*$^{-/-}$ MEFs also showed no reproducible difference in cell cycle profile or doubling times compared with wild-type cells (see Fig. S3B in the supplemental material). Furthermore, induction of DNA damage in MEFs with three separate agents (gamma-irradiation, hydroxyurea, and UV damage) did not reveal an increased sensitivity for *mPif1*$^{-/-}$ cells compared to that for wild-type cells (see Fig. S3C in the supplemental material).

Murine Pif1 associates with telomerase activity. During the characterization of the *mPif1*$^{-/-}$ mice, we observed that in vitro-expressed mPif1 interacted with recombinant telomerase activity in rabbit reticulocyte lysates and cell extracts (Fig. 4 and data not shown). The interaction of murine Pif1 occurred with both murine telomerase (Fig. 4A) and human telomerase (Fig. 4B to D). The addition of murine Pif1 to recombinant murine telomerase did not affect its activity (Fig. 4A, compare lanes 3 and 4 to lanes 7 and 8). In separate titration experiments, we found no effect of increasing levels of mPif1 on human telomerase or murine telomerase, by TRAP or a non-PCR-based elongation assay (data not shown). To further test the potential effect of mPif1 on telomerase activity, we immunoprecipitated wild-type Pif1 and a predicted helicase-inactive

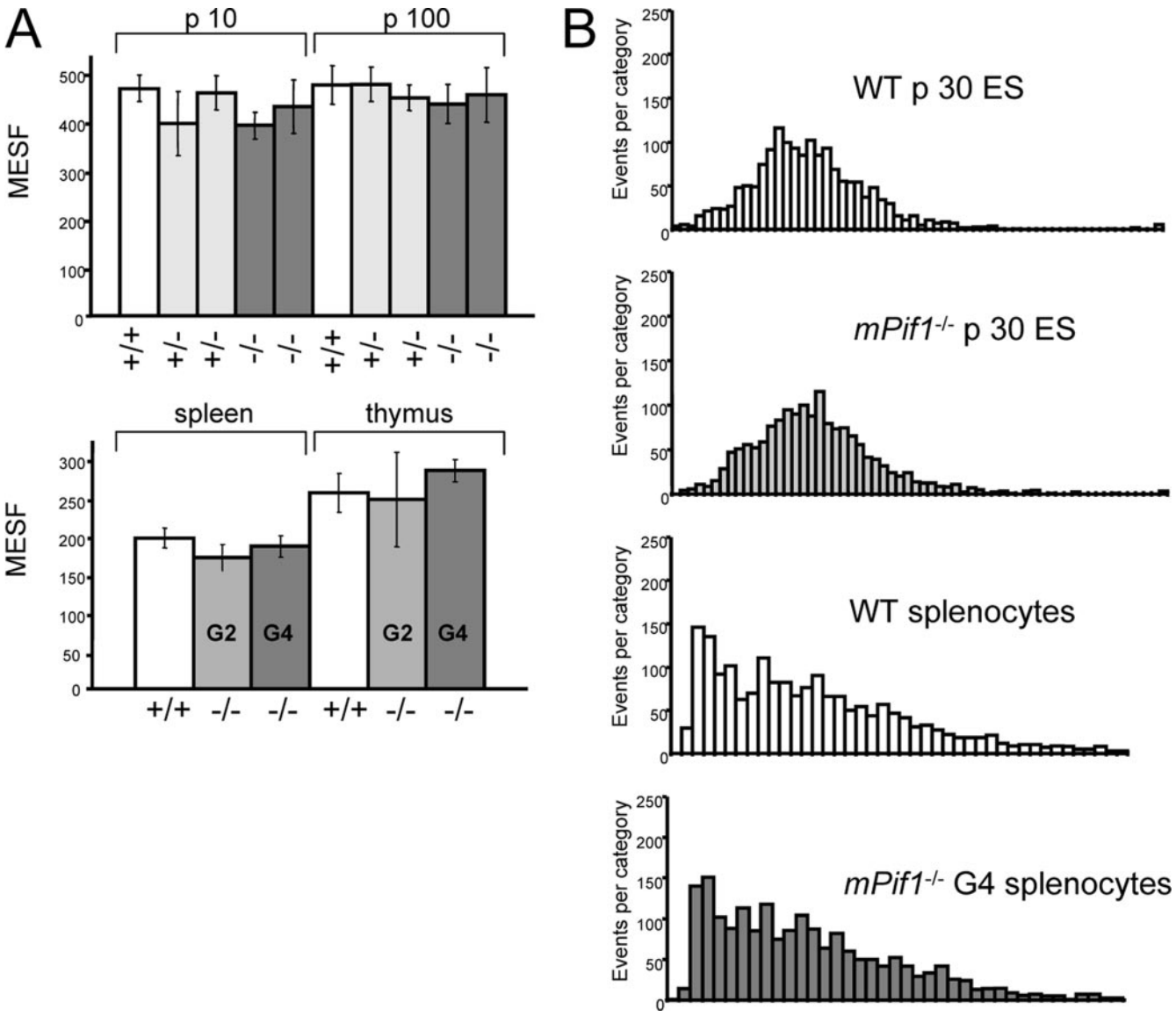

FIG. 3. Telomere length is unaltered in *mPif1*$^{-/-}$ ES cells, thymocytes, and splenocytes. (A) Flow-FISH analysis of early (p10) and late (p100) passage mouse ES cells from one wild-type and two independent *mPif1*$^{+/-}$ and *mPif1*$^{-/-}$ ES cell lines (top panel), and splenocytes and thymocytes of the indicated genotypes and generations (bottom panel). Data were pooled from at least five individual mice. Error bars represent standard deviations. MESF, molecules of equivalent soluble fluorochrome. (B) Q-FISH analyses of ES cells and activated splenocytes. Top two panels, wild-type (WT) and *mPif1* $^{-/-}$ ES cells after 30 passages. One wild-type and two independent *mPif1*$^{+/-}$ and *mPif1*$^{-/-}$ES cell clones were analyzed at passage 30, and data from one representative wild-type and *mPif1*$^{-/-}$ES cell clonal cell line are shown. Bottom two panels, activated splenocytes derived from wild-type and G4 *mPif1* $^{-/-}$ mice in a C57BL/6 genetic background At least three mice were analyzed from each generation, and results for one representative mouse are shown for each genotype. Each histogram represents 400 chromosomes (approximately 10 metaphases) from one mouse or ES cell line. The *x* axes indicate telomere fluorescence signal intensities in arbitrary units (0 for no detectable telomeric signal) for each chromosome end, and *y* axes indicate the number of ends (events) in each signal intensity category.

variant of Pif1 with both wild-type full-length hTERT and a truncation of hTERT that we showed previously was defective in processive elongation (Δ200) (5, 6). Because 100% of the telomerase in the anti-HA immunoprecipitation was associated with HA-Pif1, these results allow us to conclude that neither wild-type nor mutant mPif1 affects telomerase activity when specifically bound to TERT (Fig. 4B). Both full-length hTERT and the Δ200 hTERT mutant interacted with mPif1 in a telomerase-RNA-independent manner (Fig. 4C, lanes 3 and 4). Testing various truncations of hTERT for binding to mPif1 further emphasized the telomerase RNA independence of this interaction, since the interaction of mPif1 occurred even with hTERT mutants that cannot bind telomerase RNA (e.g., aa 401 to 1132, 536 to 1132, and 401 to 928) (Fig. 4D) (5, 6). Other truncations of hTERT failed to show a specific interaction with mPif1 (data not shown). These data define a putative novel mPif1 interaction domain for hTERT aa 536 to 928. The Pif1-telomerase interaction was specific to HA-mPif1 and not an irrelevant HA-tagged protein of a similar mass (mAif) (Fig. 4D), and the interaction was not sensitive to pretreatment with

TABLE 1. Chromosome abnormalities in MEFs and splenocytes lacking *mPif1*

Cell type	Genotype	No. of metaphases analyzed	% Aneuploidy[a]
MEFs	+/+	50	28
	+/−	50	18
	−/−	50	12
G_1 splenocytes[b]	+/+	10	30
	+/−	11	27
	−/−	10	10

[a] Percentages for metaphases with >40 or <40 chromosomes are shown. For each MEF genotype, two separate cell lines were analyzed. No fusions or chromosome breakage events were detected. On the basis of a chi-square test, only one of the two *mPif1*$^{-/-}$, MEF lines showed a significant decrease in aneuploidy ($P = 0.05$).

[b] Activated with anti-CD3 and interleukin 2 for 5 days before metaphase spread preparation.

DNase I (data not shown). Although overexpressed Pif1 could also immunoprecipitate telomerase activity in human cell extracts, the levels of endogenous mPif1 were insufficient to confirm an interaction with endogenous telomerase. However, the absence of mPif1 in cell extracts did not affect telomerase activity in vitro, since extract titrations of *mPif1*$^{-/-}$ fibroblasts or ES cells, followed by measurement of telomerase activity by the TRAP or the more quantitative, non-PCR elongation assay, revealed no differences in telomerase elongation activity (data not shown).

DISCUSSION

Similar to that of *mTert*, the expression of *mPif1* is low and appears primarily restricted to actively cycling cells and tissues. Interestingly, human *PIF1* mRNA abundance is regulated during the cell cycle, with peak expression occurring in late G_2/M (43a). Although overexpressed HA-tagged mPif1 was readily detected in the nucleus, the low levels of endogenous mPif1 were insufficient for cellular localization. Thus, we cannot exclude that endogenous Pif1 may be localized to other cellular compartments, such as the mitochondria.

Mammalian Pif1 is associated with telomerase activity when overproduced in rabbit reticulocyte lysates or in cells, and this interaction does not appear to require the telomerase RNA (this study; 43a). In *S. cerevisiae*, a recent report showed that ScPif1 precipitates the telomerase RNA *TLC1*, although it was not established whether this fraction of *TLC1* was also associated with telomerase activity (23). In that study, four separate point mutations in the region corresponding to the finger domain of Est2 (called *est2-up*) led to a telomere-lengthening phenotype that depended on nuclear Pif1 (23). We note that the human and murine TERT proteins do not contain significant sequence similarity in the region of the *est2-up* mutations; thus, it is difficult to make predictions regarding a conserved genetic interaction in this region of TERT. Interestingly, though, this study defines a putative minimal domain of hTERT that interacts with mPif1 and which overlaps with the finger domain. In contrast to results for previous in vitro studies in which purified, recombinant hPIF1 or ScPif1 was added in excess of hTERT or ScEst2 in solution (15, 75), no effect of mPif1 on telomerase activity was seen in this study, even for coimmunoprecipitations where 100% of hTERT/mTert was mPif1 associated. As our analysis of the enzymatic activity of mPif1 is still ongoing, at present we can only infer that mPif1, like its closely related ortholog hPIF1, is active under rabbit reticulocyte lysate conditions permissive for helicase activity. Regardless of the catalytic status of mPif1, we show for the first time that mPif1 can bind to mammalian telomerase in vitro and that this interaction does not depend on the catalytic competence of mPif1. Therefore, it appears that a telomerase-Pif1 interaction is conserved between mammals and *S. cerevisiae*.

It is possible that the distinct biochemical properties of murine telomerase may mask any effect of Pif1 unwinding activity. Murine telomerase is much less processive than human telomerase (56), and unlike *S. cerevisiae*, telomerase can dissociate from its substrate (19, 55). The inherent capacity of mTert to release a telomeric substrate could thereby render the unwinding activity of Pif1 redundant. The association of Pif1 with telomerase may become important only in specific circumstances, such as the recruitment of telomerase to broken chromosome ends. Recently, human PIF1 was demonstrated to exhibit an ATP-dependent unwinding activity (29); however, the precise substrate specificities of human and murine Pif1, compared to that of ScPif1, remain to be established.

Consistent with the lack of effect of mPif1 on telomerase activity in vitro or in *mPif1*$^{-/-}$ extracts, we observed no reproducible change in telomere length in the absence of *mPif1* in vivo. Blasco and colleagues also analyzed an independently derived *mPif1*$^{-/-}$ murine strain and found no observable difference in average telomere lengths or cell viability in response to DNA damage (Maria Blasco, personal communication). In *S. cerevisiae*, the absence of nuclear Pif1 leads to telomere lengthening (76). In *mPif1*-deficient mice that already possess long telomeres, it is possible that further telomere lengthening could be offset by the intrastrand excision of telomeric DNA—a phenomenon observed in *S. cerevisiae* strains with very long telomeres (12, 40) and in human cells deficient in telomere capping (73). It will be interesting to determine whether telomere lengthening in the absence of *mPif1* occurs in other genetic backgrounds, particularly in *mTert* heterozygous animals or outbred murine strains, which possess a shorter average telomere length but retain telomerase activity (22, 38).

The lack of an obvious phenotype in the absence of *mPif1* makes it difficult to conclude whether mPif1 is orthologous to *S. cerevisiae* Pif1 or Rrm3. Homology searches of the murine database did not reveal any other genes with significant similarity to Pif1 or Rrm3. In addition, a search for putative homologs of the known Rrm3-interacting protein Def1, which plays a role in telomere length maintenance (18), did not reveal any proteins with obvious sequence similarity. It is possible that conservation of Pif1 function does not extend to telomere DNA replication in all organisms; however, this conclusion would appear inconsistent with the observation that Pif1 interacts with telomerase (our study; 43a) and with a recent report that human Pif1 is telomere associated (75). Other characterized mammalian helicases do not exhibit extensive redundancy in vivo. For example, the five known RecQ helicases (Wrn, Blm, RecQ4, RecQL, and RecQ5b) and XPB/ERCC3 (implicated in xeroderma pigmentosum and Cockayne

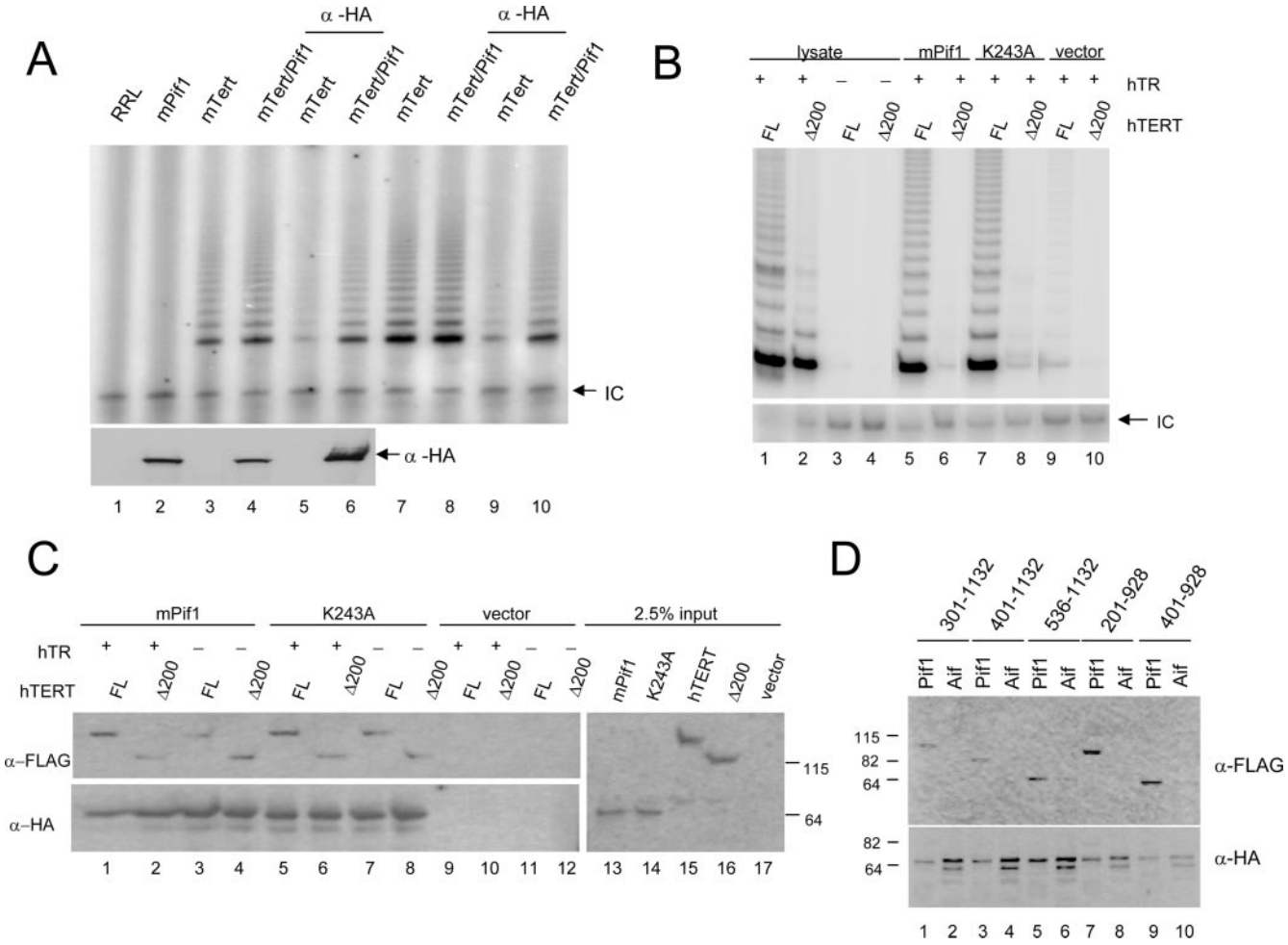

FIG. 4. In vitro interaction between telomerase and mPif1. (A) Murine telomerase interacts with mPif1. The top panel shows results for TRAP assays from rabbit reticulocyte lysates (RRLs) containing reconstituted murine telomerase (mTert). Lanes 1 to 4, TRAP assays from 0.5 μl of an RRL reconstituted with the following: no vector (RRL) (lane 1), HA-tagged wild-type mPif1 (lane 2), wild-type mTert (lane 3), or mPif1 mixed with mTert (lane 4). Lanes 5 and 6 show results for TRAP assays from anti-HA (α-HA) immunoprecipitations (2 μl) of the same lysates as those used for lanes 3 and 4, respectively. Lanes 7 to 10, duplicates of lanes 3 to 6. The expression of HA-tagged mPif1 was confirmed by anti-HA Western blotting (bottom panel). In this experiment, mTert was untagged and undetectable with available antibodies. All TRAP reaction mixtures contained an internal control product to indicate PCR amplification (IC) (arrow at right). (B and C) Murine Pif1 interacts with human telomerase. (B) TRAP analysis of 0.5 μl of the RRLs from Fig. 4C, containing full-length (FL) or hTERT missing the first 200 aa (Δ200), either with (lanes 1 and 2) or without (lanes 3 and 4) telomerase RNA (+hTR) and after immunoprecipitation (2 μl) of hTERT plus hTR onto anti-HA resin (lanes 5 to 10) in the presence of wild-type mPif1 (mPif1), a mutant mPif1 predicted to possess no helicase activity (K243A; equivalent to K234A in hPIF1 (15), or vector alone (vector) (lanes 5 to 10). All TRAP reaction mixtures contained an internal control product to indicate PCR amplification (IC) (arrow at right). (C) FLAG-tagged human TERT, the full-length (FL) or a mutant version missing the first 200 aa (Δ200), was reconstituted in RRL in the presence (+) or absence (−) of the telomerase RNA (hTR) and mixed with the following: lysate alone (vector) (lanes 9 to 12), HA-tagged mPif1 (lanes 1 to 4), or HA-tagged mPif1-K243A (predicted to possess no helicase activity) (K243A) (lanes 5 to 8). The mixtures were then immunoprecipitated onto an anti-HA antibody-containing resin, resolved by sodium dodecyl sulfate-polyacrylamide gel electrophoresis, transferred to a membrane, and probed with either anti-FLAG antibody (to detect hTERT) (top panel) or anti-HA antibody (to detect Pif1) (bottom panel). To determine the efficiency of the RRL reaction, approximately 2.5% of each input RRL was analyzed on the same Western blot as that shown on the left (right panel) (lanes 13 to 17). This blot was serially probed first with anti-FLAG antibody and then with anti-HA antibody; thus, both HA-mPif1 and FLAG-hTERT are visualized simultaneously. (D) Mapping of the mPif1-TERT interaction. A series of FLAG-tagged TERT deletions were tested in RRL for their ability to coimmunoprecipitate HA-tagged mPif1 or mAif onto anti-HA agarose beads. Blots were probed serially for anti-FLAG (top panel) and anti-HA (bottom panel). The amino acids comprising each hTERT deletion construct are indicated above. Note that HA-mAif (predicted mass, 72.9 kDa) migrates as a doublet at a position similar to that of HA-mPif1 (predicted mass, 71 kDa).

syndrome) show limited redundancy in rescuing p53-dependent apoptosis in Bloom-deficient cells (63); however, mutations in each helicase gene have distinct phenotypes in genome stability and DNA replication and repair in vivo and all are separately implicated in human disease (8, 34, 49, 62).

It is quite plausible that mammalian Pif1 function is important for other types of DNA damage not yet examined. For example, loss-of-function studies of the BRCA1-interacting DNA helicase, BACH1, revealed a role in DNA repair distinct from that of BRCA1, and despite sensitivity to cisplatin and mitomycin C, *BACH1*-deficient cells are relatively unaffected by treatment with UV, X rays, or methyl methanesulfonate

(16, 53). To test the role of mPif1 in chromosome healing, we plan to make use of an elegant system developed by Murnane and colleagues, in which a telomere can be cleaved via a unique I-SceI site integrated into the subtelomeric DNA of one chromosome (39, 64). Since deletion of *ScPIF1* leads to an increase in mitochondrial DNA point mutations, particularly after oxidative damage (21, 51, 52, 67), it is also possible mPif1 plays a nonessential role in mitochondrial genome stability. Although Sc*rrm3*Δ cells do not exhibit changes in GCR or mitochondrial genome stability, these cells do exhibit genetic instability, presumably due to replication fork pausing at specific chromosomal loci, such as the ribosomal DNA locus (31, 32, 45, 59, 68, 69). Sc*RRM3* and Sc*PIF1* exhibit genetic interactions (including synthetic lethality) with many gene products required in DNA replication and S-phase checkpoint arrest (1, 2, 17, 50, 58, 59, 69, 71). Thus, additional inactivation of other DNA helicases involved in DNA replication or repair or proteins essential for the S-phase checkpoint may yet reveal an interesting phenotype in $mPif^{-/-}$ animals.

ACKNOWLEDGMENTS

We thank Maria Mateyak, Virginia Zakian, John Murnane, and Maria Blasco for sharing unpublished results. We thank David Sealey for the chromatin immunoprecipitation analysis of mPif1 (unpublished) and for comments on the manuscript. We thank Mike Tyers, Daniel Durocher, and Carol Greider for advice and comments.

We thank Tak W. Mak for funding Andrew Wakeham's contribution. This study was funded by a grant from the NIH/NIA Longevity Assurance Genes Program (AG024398) and National Cancer Institute of Canada Research grant no. 15072 (using funds from the Canadian Cancer Society) to L.H.

REFERENCES

1. **Aroya, S. B., and M. Kupiec.** 2005. The Elg1 replication factor C-like complex: a novel guardian of genome stability. DNA Repair (Amsterdam) **4:**409–417.
2. **Azam, M., J. Y. Lee, V. Abraham, R. Chanoux, K. A. Schoenly, and F. B. Johnson.** 2006. Evidence that the S.cerevisiae Sgs1 protein facilitates recombinational repair of telomeres during senescence. Nucleic Acids Res. **34:**506–516.
3. **Baerlocher, G. M., J. Mak, T. Tien, and P. M. Lansdorp.** 2002. Telomere length measurement by fluorescence in situ hybridization and flow cytometry: tips and pitfalls. Cytometry **47:**89–99.
4. **Bayani, J., M. Zielenska, P. Marrano, Y. Kwan Ng, M. D. Taylor, V. Jay, J. T. Rutka, and J. A. Squire.** 2000. Molecular cytogenetic analysis of medulloblastomas and supratentorial primitive neuroectodermal tumors by using conventional banding, comparative genomic hybridization, and spectral karyotyping. J. Neurosurg. **93:**437–448.
5. **Beattie, T. L., W. Zhou, M. O. Robinson, and L. Harrington.** 2001. Functional multimerization of the human telomerase reverse transcriptase. Mol. Cell. Biol. **21:**6151–6160.
6. **Beattie, T. L., W. Zhou, M. O. Robinson, and L. Harrington.** 2000. Polymerization defects within human telomerase are distinct from telomerase RNA and TEP1 binding. Mol. Biol. Cell **11:**3329–3340.
7. **Beattie, T. L., W. Zhou, M. O. Robinson, and L. Harrington.** 1998. Reconstitution of human telomerase activity in vitro. Curr. Biol. **8:**177–180.
8. **Bennett, R. J., and J. L. Keck.** 2004. Structure and function of RecQ DNA helicases. Crit. Rev. Biochem. Mol. Biol. **39:**79–97.
9. **Bertuch, A. A., and V. Lundblad.** 2003. Which end: dissecting Ku's function at telomeres and double-strand breaks. Genes Dev. **17:**2347–2350.
10. **Bessler, J. B., J. Z. Torredagger, and V. A. Zakian.** 2001. The Pif1p subfamily of helicases: region-specific DNA helicases? Trends Cell Biol. **11:**60–65.
11. **Bessler, J. B., and V. A. Zakian.** 2004. The amino terminus of the Saccharomyces cerevisiae DNA helicase Rrm3p modulates protein function altering replication and checkpoint activity. Genetics **168:**1205–1218.
12. **Bhattacharyya, M. K., and A. J. Lustig.** 2006. Telomere dynamics in genome stability. Trends Biochem. Sci. **31:**114–122.
13. **Biek, D. P., and S. N. Cohen.** 1986. Identification and characterization of *recD*, a gene affecting plasmid maintenance and recombination in *Escherichia coli*. J. Bacteriol. **167:**594–603.
14. **Blasco, M. A., H. W. Lee, M. P. Hande, E. Samper, P. M. Lansdorp, R. A. DePinho, and C. W. Greider.** 1997. Telomere shortening and tumor formation by mouse cells lacking telomerase RNA. Cell **91:**25–34.
15. **Boule, J. B., L. R. Vega, and V. A. Zakian.** 2005. The yeast Pif1p helicase removes telomerase from telomeric DNA. Nature **438:**57–61.
16. **Bridge, W. L., C. J. Vandenberg, R. J. Franklin, and K. Hiom.** 2005. The BRIP1 helicase functions independently of BRCA1 in the Fanconi anemia pathway for DNA crosslink repair. Nat. Genet. **37:**953–957.
17. **Budd, M. E., C. C. Reis, S. Smith, K. Myung, and J. L. Campbell.** 2006. Evidence suggesting that Pif1 helicase functions in DNA replication with the Dna2 helicase/nuclease and DNA polymerase delta. Mol. Cell. Biol. **26:**2490–2500.
18. **Chen, Y. B., C. P. Yang, R. X. Li, R. Zeng, and J. Q. Zhou.** 2005. Def1p is involved in telomere maintenance in budding yeast. J. Biol. Chem. **280:**24784–24791.
19. **Cohn, M., and E. H. Blackburn.** 1995. Telomerase in yeast. Science **269:**396–400.
20. **Ding, H., M. Schertzer, X. Wu, M. Gertsenstein, S. Selig, M. Kammori, R. Pourvali, S. Poon, I. Vulto, E. Chavez, P. P. Tam, A. Nagy, and P. M. Lansdorp.** 2004. Regulation of murine telomere length by Rtel: an essential gene encoding a helicase-like protein. Cell **117:**873–886.
21. **Doudican, N. A., B. Song, G. S. Shadel, and P. W. Doetsch.** 2005. Oxidative DNA damage causes mitochondrial genomic instability in *Saccharomyces cerevisiae*. Mol. Cell. Biol. **25:**5196–5204.
22. **Erdmann, N., Y. Liu, and L. Harrington.** 2004. Distinct dosage requirements for the maintenance of long and short telomeres in mTert heterozygous mice. Proc. Natl. Acad. Sci. USA **101:**6080–6085.
23. **Eugster, A., C. Lanzuolo, M. Bonneton, P. Luciano, A. Pollice, J. F. Pulitzer, E. Stegberg, A. S. Berthiau, K. Forstemann, Y. Corda, J. Lingner, V. Geli, and E. Gilson.** 2006. The finger subdomain of yeast telomerase cooperates with Pif1p to limit telomere elongation. Nat. Struct. Mol. Biol. **13:**734–739.
24. **Evans, S. K., and V. Lundblad.** 2000. Positive and negative regulation of telomerase access to the telomere. J. Cell Sci. **113:**3357–3364.
25. **Fisher, T. S., and V. A. Zakian.** 2005. Ku: a multifunctional protein involved in telomere maintenance. DNA Repair (Amsterdam) **4:**1215–1226.
26. **Gorbalenya, A. E., and E. V. Koonin.** 1993. Helicases: amino acid sequence comparisons and structure-function relationships. Curr. Opin. Struct. Biol. **3:**419–429.
27. **Grandin, N., C. Damon, and M. Charbonneau.** 2001. Ten1 functions in telomere end protection and length regulation in association with Stn1 and Cdc13. EMBO J. **20:**1173–1183.
28. **Hakem, R., J. L. de la Pompa, C. Sirard, R. Mo, M. Woo, A. Hakem, A. Wakeham, J. Potter, A. Reitmair, F. Billia, E. Firpo, C. C. Hui, J. Roberts, J. Rossant, and T. W. Mak.** 1996. The tumor suppressor gene Brca1 is required for embryonic cellular proliferation in the mouse. Cell **85:**1009–1023.
29. **Huang, Y., D. H. Zhang, and J. Q. Zhou.** 2006. Characterization of ATPase activity of recombinant human Pif1. Acta Biochim. Biophys. Sin. (Shanghai) **38:**335–341.
30. **Hug, N., and J. Lingner.** 2006. Telomere length homeostasis. Chromosoma **115:**413–425.
31. **Ivessa, A. S., B. A. Lenzmeier, J. B. Bessler, L. K. Goudsouzian, S. L. Schnakenberg, and V. A. Zakian.** 2003. The Saccharomyces cerevisiae helicase Rrm3p facilitates replication past nonhistone protein-DNA complexes. Mol. Cell **12:**1525–1536.
32. **Ivessa, A. S., J. Q. Zhou, V. P. Schulz, E. K. Monson, and V. A. Zakian.** 2002. Saccharomyces Rrm3p, a 5′ to 3′ DNA helicase that promotes replication fork progression through telomeric and subtelomeric DNA. Genes Dev. **16:**1383–1396.
33. **Ivessa, A. S., J. Q. Zhou, and V. A. Zakian.** 2000. The Saccharomyces Pif1p DNA helicase and the highly related Rrm3p have opposite effects on replication fork progression in ribosomal DNA. Cell **100:**479–489.
34. **Khakhar, R. R., J. A. Cobb, L. Bjergbaek, I. D. Hickson, and S. M. Gasser.** 2003. RecQ helicases: multiple roles in genome maintenance. Trends Cell Biol. **13:**493–501.
35. **Kim, N. W., M. A. Piatyszek, K. R. Prowse, C. B. Harley, M. D. West, P. L. Ho, G. M. Coviello, W. E. Wright, S. L. Weinrich, and J. W. Shay.** 1994. Specific association of human telomerase activity with immortal cells and cancer. Science **266:**2011–2015.
36. **Korolev, S., J. Hsieh, G. H. Gauss, T. M. Lohman, and G. Waksman.** 1997. Major domain swiveling revealed by the crystal structures of complexes of E. coli Rep helicase bound to single-stranded DNA and ADP. Cell **90:**635–647.
37. **Lahaye, A., H. Stahl, D. Thines-Sempoux, and F. Foury.** 1991. PIF1: a DNA helicase in yeast mitochondria. EMBO J. **10:**997–1007.
38. **Liu, Y., H. Kha, M. Ungrin, M. O. Robinson, and L. Harrington.** 2002. Preferential maintenance of critically short telomeres in mammalian cells heterozygous for mTert. Proc. Natl. Acad. Sci. USA **99:**3597–3602.
39. **Lo, A. W., C. N. Sprung, B. Fouladi, M. Pedram, L. Sabatier, M. Ricoul, G. E. Reynolds, and J. P. Murnane.** 2002. Chromosome instability as a result of double-strand breaks near telomeres in mouse embryonic stem cells. Mol. Cell. Biol. **22:**4836–4850.
40. **Lustig, A. J.** 2003. Clues to catastrophic telomere loss in mammals from yeast telomere rapid deletion. Nat. Rev. Genet. **4:**916–923.
41. **Lydall, D.** 2003. Hiding at the ends of yeast chromosomes: telomeres, nucleases and checkpoint pathways. J. Cell Sci. **116:**4057–4065.

42. **Mangahas, J. L., M. K. Alexander, L. L. Sandell, and V. A. Zakian.** 2001. Repair of chromosome ends after telomere loss in Saccharomyces. Mol. Biol. Cell **12:**4078–4089.
43. **Marchler-Bauer, A., J. B. Anderson, P. F. Cherukuri, C. DeWeese-Scott, L. Y. Geer, M. Gwadz, S. He, D. I. Hurwitz, J. D. Jackson, Z. Ke, C. J. Lanczycki, C. A. Liebert, C. Liu, F. Lu, G. H. Marchler, M. Mullokandov, B. A. Shoemaker, V. Simonyan, J. S. Song, P. A. Thiessen, R. A. Yamashita, J. J. Yin, D. Zhang, and S. H. Bryant.** 2005. CDD: a Conserved Domain Database for protein classification. Nucleic Acids Res. **33:**D192–D196.

43a. **Mateyak, M. K., and V. A. Zakian.** 2006. Human PIF1 helicase is cell cycle regulated and associates with telomerase. Cell Cycle **5:**2796–2804.

44. **Mitelman, F.** 1995. An international system for human cytogenetic nomenclature. S. Karger, Basel, Switzerland.
45. **Mohanty, B. K., N. K. Bairwa, and D. Bastia.** 2006. The Tof1p-Csm3p protein complex counteracts the Rrm3p helicase to control replication termination of Saccharomyces cerevisiae. Proc. Natl. Acad. Sci. USA **103:**897–902.
46. **Myers, R. S., and F. W. Stahl.** 1994. Chi and the RecBC D enzyme of Escherichia coli. Annu. Rev. Genet. **28:**49–70.
47. **Myung, K., C. Chen, and R. D. Kolodner.** 2001. Multiple pathways cooperate in the suppression of genome instability in Saccharomyces cerevisiae. Nature **411:**1073–1076.
48. **Myung, K., V. Pennaneach, E. S. Kats, and R. D. Kolodner.** 2003. Saccharomyces cerevisiae chromatin-assembly factors that act during DNA replication function in the maintenance of genome stability. Proc. Natl. Acad. Sci. USA **100:**6640–6645.
49. **Oh, K. S., S. G. Khan, N. G. Jaspers, A. Raams, T. Ueda, A. Lehmann, P. S. Friedmann, S. Emmert, A. Gratchev, K. Lachlan, A. Lucassan, C. C. Baker, and K. H. Kraemer.** 2006. Phenotypic heterogeneity in the XPB DNA helicase gene (ERCC3): xeroderma pigmentosum without and with Cockayne syndrome. Hum. Mutat. **27:**1092–1103
50. **Ooi, S. L., D. D. Shoemaker, and J. D. Boeke.** 2003. DNA helicase gene interaction network defined using synthetic lethality analyzed by microarray. Nat. Genet. **35:**277–286.
51. **O'Rourke, T. W., N. A. Doudican, M. D. Mackereth, P. W. Doetsch, and G. S. Shadel.** 2002. Mitochondrial dysfunction due to oxidative mitochondrial DNA damage is reduced through cooperative actions of diverse proteins. Mol. Cell. Biol. **22:**4086–4093.
52. **O'Rourke, T. W., N. A. Doudican, H. Zhang, J. S. Eaton, P. W. Doetsch, and G. S. Shadel.** 2005. Differential involvement of the related DNA helicases Pif1p and Rrm3p in mtDNA point mutagenesis and stability. Gene **354:** 86–92.
53. **Peng, M., R. Litman, Z. Jin, G. Fong, and S. B. Cantor.** 2006. BACH1 is a DNA repair protein supporting BRCA1 damage response. Oncogene **25:** 2245–2253.
54. **Pennaneach, V., C. D. Putnam, and R. D. Kolodner.** 2006. Chromosome healing by de novo telomere addition in Saccharomyces cerevisiae. Mol. Microbiol. **59:**1357–1368.
55. **Prescott, J., and E. H. Blackburn.** 1997. Functionally interacting telomerase RNAs in the yeast telomerase complex. Genes Dev. **11:**2790–2800.
56. **Prowse, K. R., A. A. Avilion, and C. W. Greider.** 1993. Identification of a nonprocessive telomerase activity from mouse cells. Proc. Natl. Acad. Sci. USA **90:**1493–1497.
57. **Rufer, N., W. Dragowska, G. Thornbury, E. Roosnek, and P. M. Lansdorp.** 1998. Telomere length dynamics in human lymphocyte subpopulations measured by flow cytometry. Nat. Biotechnol. **16:**743–747.
58. **Ryu, G. H., H. Tanaka, D. H. Kim, J. H. Kim, S. H. Bae, Y. N. Kwon, J. S. Rhee, S. A. MacNeill, and Y. S. Seo.** 2004. Genetic and biochemical analyses of Pfh1 DNA helicase function in fission yeast. Nucleic Acids Res. **32:**4205–4216.
59. **Schmidt, K. H., and R. D. Kolodner.** 2004. Requirement of Rrm3 helicase for repair of spontaneous DNA lesions in cells lacking Srs2 or Sgs1 helicase. Mol. Cell. Biol. **24:**3213–3226.
60. **Schrock, E., T. Veldman, H. Padilla-Nash, Y. Ning, J. Spurbeck, S. Jalal, L. G. Shaffer, P. Papenhausen, C. Kozma, M. C. Phelan, E. Kjeldsen, S. A. Schonberg, P. O'Brien, L. Biesecker, S. du Manoir, and T. Ried.** 1997. Spectral karyotyping refines cytogenetic diagnostics of constitutional chromosomal abnormalities. Hum. Genet. **101:**255–262.
61. **Schulz, V. P., and V. A. Zakian.** 1994. The saccharomyces PIF1 DNA helicase inhibits telomere elongation and de novo telomere formation. Cell **76:**145–155.
62. **Sharma, S., K. M. Doherty, and R. M. Brosh, Jr.** 2006. Mechanisms of RecQ helicases in pathways of DNA metabolism and maintenance of genomic stability. Biochem. J. **398:**319–337.
63. **Spillare, E. A., X. W. Wang, C. von Kobbe, V. A. Bohr, I. D. Hickson, and C. C. Harris.** 2006. Redundancy of DNA helicases in p53-mediated apoptosis. Oncogene **25:**2119–2123.
64. **Sprung, C. N., G. Afshar, E. A. Chavez, P. Lansdorp, L. Sabatier, and J. P. Murnane.** 1999. Telomere instability in a human cancer cell line. Mutat. Res. **429:**209–223.
65. **Stellwagen, A. E., Z. W. Haimberger, J. R. Veatch, and D. E. Gottschling.** 2003. Ku interacts with telomerase RNA to promote telomere addition at native and broken chromosome ends. Genes Dev. **17:**2384–2395.
66. **Taggart, A. K., and V. A. Zakian.** 2003. Telomerase: what are the Est proteins doing? Curr. Opin. Cell Biol. **15:**275–280.
67. **Taylor, S. D., H. Zhang, J. S. Eaton, M. S. Rodeheffer, M. A. Lebedeva, W. O'Rourke, T. W. Siede, and G. S. Shadel.** 2005. The conserved Mec1/Rad53 nuclear checkpoint pathway regulates mitochondrial DNA copy number in Saccharomyces cerevisiae. Mol. Biol. Cell **16:**3010–3018.
68. **Torres, J. Z., J. B. Bessler, and V. A. Zakian.** 2004. Local chromatin structure at the ribosomal DNA causes replication fork pausing and genome instability in the absence of the S. cerevisiae DNA helicase Rrm3p. Genes Dev. **18:** 498–503.
69. **Torres, J. Z., S. L. Schnakenberg, and V. A. Zakian.** 2004. *Saccharomyces cerevisiae* Rrm3p DNA helicase promotes genome integrity by preventing replication fork stalling: viability of *rrm3* cells requires the intra-S-phase checkpoint and fork restart activities. Mol. Cell. Biol. **24:**3198–3212.
70. **Van Dyck, E., F. Foury, B. Stillman, and S. J. Brill.** 1992. A single-stranded DNA binding protein required for mitochondrial DNA replication in S. cerevisiae is homologous to E. coli SSB. EMBO J. **11:**3421–3430.
71. **Wagner, M., G. Price, and R. Rothstein.** 2006. The absence of Top3 reveals an interaction between the Sgs1 and Pif1 DNA helicases in Saccharomyces cerevisiae. Genetics **174:**555–573
72. **Wahle, E., and W. Keller.** 1996. The biochemistry of polyadenylation. Trends Biochem. Sci. **21:**247–250.
73. **Wang, R. C., A. Smogorzewska, and T. de Lange.** 2004. Homologous recombination generates T-loop-sized deletions at human telomeres. Cell **119:**355–368.
74. **Williams, B., and A. J. Lustig.** 2003. The paradoxical relationship between NHEJ and telomeric fusion. Mol. Cell **11:**1125–1126.
75. **Zhang, D. H., B. Zhou, Y. Huang, L. X. Xu, and J. Q. Zhou.** 2006. The human Pif1 helicase, a potential Escherichia coli RecD homologue, inhibits telomerase activity. Nucleic Acids Res. **34:**1393–1404.
76. **Zhou, J., E. K. Monson, S. C. Teng, V. P. Schulz, and V. A. Zakian.** 2000. Pif1p helicase, a catalytic inhibitor of telomerase in yeast. Science **289:**771–774.
77. **Zhou, J. Q., H. Qi, V. P. Schulz, M. K. Mateyak, E. K. Monson, and V. A. Zakian.** 2002. Schizosaccharomyces pombe pfh1+ encodes an essential 5′ to 3′ DNA helicase that is a member of the PIF1 subfamily of DNA helicases. Mol. Biol. Cell **13:**2180–2191.
78. **Zijlmans, J. M., U. M. Martens, S. S. Poon, A. K. Raap, H. J. Tanke, R. K. Ward, and P. M. Lansdorp.** 1997. Telomeres in the mouse have large interchromosomal variations in the number of T2AG3 repeats. Proc. Natl. Acad. Sci. USA **94:**7423–7428.